Influence of thyroid volume reduction on absorbed dose in ^{131}I therapy studied by using Geant4 Monte Carlo simulation

Ziaur Rahman[1] Sikander M Mirza[2] Waheed Arshed[1] Nasir M Mirza[2] Waheed Ahmed[1]

[1] Health Physics Division, Pakistan Institute of Nuclear Science and Technology, Nilore, Islamabad 45650, Pakistan
[2] Department of Physics and Applied Mathematics, Pakistan Institute of Engineering and Applied Sciences, Nilore, Islamabad 45650, Pakistan

Abstract: A simulation study has been performed to quantify the effect of volume reduction on the thyroid absorbed dose per decay and to investigate the variation of energy deposition per decay due to β- and γ-activity of ^{131}I with volume/mass of thyroid, for water, ICRP- and ICRU-soft tissue taken as thyroid material. A Monte Carlo model of the thyroid, in the Geant4 radiation transport simulation toolkit was constructed to compute the β- and γ-absorbed dose in the simulated thyroid phantom for various values of its volume. The effect of the size and shape of the thyroid on energy deposition per decay has also been studied by using spherical, ellipsoidal and cylindrical models for the thyroid and varying its volume in 1–25 cm^3 range. The relative differences of Geant4 results for different models with each other and MCNP results lie well below 1.870%. The maximum relative difference among the Geant4 estimated results for water with ICRP and ICRU soft tissues is not more than 0.225%. S-values for ellipsoidal, spherical and cylindrical thyroid models were estimated and the relative difference with published results lies within 3.095%. The absorbed fraction values for beta particles show a good agreement with published values within 2.105% deviation. The Geant4 based simulation results of absorbed fractions for gammas again show a good agreement with the corresponding MCNP and EGS4 results (±6.667%) but have 29.032% higher values than that of MIRD calculated values. Consistent with previous studies, the reduction of the thyroid volume is found to have a substantial effect on the absorbed dose. Geant4 simulations confirm dose dependence on the volume/mass of thyroid in agreement with MCNP and EGS4 computed values but are substantially different from MIRD8 data. Therefore, inclusion of size/mass dependence is indicated for ^{131}I radiotherapy of the thyroid.

Key words: mean absorbed dose rate, Geant4, Monte Carlo simulation and ^{131}I therapy

PACS: 87.55.dk, 87.53.Bn, 87.55.K **DOI:** 10.1088/1674-1137/38/5/056201

1 Introduction

The treatment of differentiated thyroid cancer and thyrotoxicosis has become quite successful since the introduction of the ^{131}I radiotherapy technique over six decades ago. The associated radiation damage has always been of concern to practitioners in this area [1]. Various other therapeutical modalities have been noted to have only a modest effect on advanced differentiated thyroid cancer [2]. In earlier studies, severe radiation damage to the thyroid has been reported due to high imparted dose from radioactive materials. Limiting side exposure of sensitive organs that are susceptible to radiation is also essential. The impairment of salivary glands in post DTC radioiodine therapy is a severe side effect [3]. Thyroid dose is also of current interest in various high dose applications, including CT examination, and controversy persists regarding the types of patients and the recommended dose of radioiodine [4]. The unpredictability of success of radioiodine therapy in the case of hyperthyroidism has been linked with waste of radiations before reaching the target cells. As a corrective measure, precise assessment of absorbed dose to patient-specific thyroid micro-architecture based on size involved has been recommended [5].

The observed variation of thyroid volume during treatment adds to the gravity of the situation. For the ablation of remnant thyroid tissue after surgery, the standard amount of radioiodine administered varies, typically in the 1.1–3.7 GBq range. The use of any un-optimized 'standard' value entails the risk of either exceeding safety limits or under-dosing a patient [6]. In the latter case, there is an associated risk of recurrence of disease. Coupled with this, there is prevalent practice of using empiric fixed activities of ^{131}I for treatment of advanced stages of differentiated thyroid cancer [6, 7]. This approach clearly violates the safety principle of delivering maximum allowable safe absorbed dose. No attempt is made to

Received 19 June 2013

minimize the side effects of radiotherapy in this case.

For this purpose, many authors have developed theoretical algorithms/ procedures for the calculation of the radiation absorbed dose to a target organ, most of them are based on the basic absorbed dose rate equation of MIRD [8]. Besides the theoretical approach, Monte Carlo simulations have also emerged as a highly effective tool for dosimetry among medical physicists working in the field of nuclear medicine, especially for optimizing routinely used devices, such as detectors, collimators and shields, and evaluating the exposure radiation dose in diagnostic and therapeutic protocols [5, 9–11]. Recently, particular attention has been shown towards the use of the Monte Carlo simulations in studying beta and gamma emitting radionuclide's that are used for treatment of various forms of cancer and other diseases. Meo et al. [10] have used Geant4 MC simulation code for measuring dose rate from patients administered with ^{90}Y-labeled radiopharmaceuticals. In 1994, Siegel and Stabin evaluated the absorbed fractions for electron and beta sources uniformly distributed within spheres of various sizes [12] in the energy ranges of 0.062 to 1.428 MeV and 0.025 to 4 MeV, respectively, using the methodology developed by Berger [13]. Afterwards, in 2000 Stabin and Konijnenberg re-evaluated these values using two different Monte Carlo codes, EGS4 and MCNP-4B, showing some interesting discrepancies between the results [14].

In almost all of the methods described above, the mass or volume of the target organ is typically kept constant over the dose delivery time. However, in the case of radioiodine treatment of hyperthyroidism, many authors have reported a thyroid volume reduction (of up to 70%–80%) during therapy [15–17]. Since the treatment dose is dependent on the volume/mass of the target organ, the accurate measurement of volume of thyroid is essential for efficient therapy. In this regard, Traino et al. have studied the influence of the volume reduction on the calculation of the absorbed dose to the thyroid using a mathematical model [18]. Similarly, in recent studies, researchers [11] have used Monte Carlo simulations to study the influence of change in thyroid volume on the energy deposition from ^{131}I. The remnant tissue mass dependency after ^{131}I ablation therapy for the thyroid absorbed dose was studied using Monte Carlo simulations employing standard geometrical models [19]. They found 11%–37% over-estimation of S-values when spherical geometries were employed and they recommended usage of precise remnant mass and size values for accurate thyroid dosimetry.

In this study, the effect of the mass reduction of the thyroid during ^{131}I therapy on the calculation of absorbed dose is estimated using Geant4 Monte Carlo simulation code. Further simulations have been carried for water, ICRP and ICRU tissue as thyroid material and results are compared. In addition, various thyroid geometries (shape) including spheres, cylinders and ellipsoids have been considered and the respective results are compared with published data. For ^{131}I, β- and γ-absorbed fraction and S-values for various geometries of thyroid are estimated and the results have been compared with already published results. The dependence of specific energy deposition per decay (ξ), energy deposition per decay (ϵ) and activity-to-dose-rate conversion factor (K) on thyroid volume (η) have been fitted using non-linear least-square fitting method and the results are presented.

2 Materials and methods

In this study the following MIRD schema has been used for estimation of absorbed dose to thyroid [8]:

$$\dot{D}_{\mathrm{T}}=\frac{kA_{\mathrm{s}}}{m_{\mathrm{T}}}\sum_{\mathrm{i}}y_{\mathrm{i}}E_{\mathrm{i}}\varphi_{\mathrm{i}}, \tag{1}$$

where $\dot{D}$ absorbed dose rate to a target region of interest (mGy/hr); A_{s} is activity (MBq) in the source region; y_{i} is number of radiations with energy E_{i} (MeV) emitted per nuclear transition; φ_{i} is fraction of energy emitted in a source region that is absorbed in a target region; and, m_{T} is mass of the target region (kg) and k is proportionality constant (Gy·kg/MBq·hr·MeV).

The Geant4 Monte Carlo simulation tool kit has been used in this study to track the particles. Geant4 simulates hadronic, electromagnetic and optical processes. A key feature of Geant4 is that it offers lower energy physics models, namely PENELOPE, LIVERMORE, besides the STANDARD one, for accurate simulation of low energy processes [20]. The accuracy of Geant4, comparison of the electromagnetic process and physics models have been investigated by several authors [21].

Geant4 simulations have been carried out to calculate the energy deposition per decay for beta- and gamma-rays of ^{131}I for ellipsoidal, spherical and cylindrical thyroid models of various sizes, ranging from 1–25 cm^3, using water, ICRP and ICRU soft tissues as thyroid material. The principal axes for ellipsoidal and cylindrical models were taken at the ratio of 1/1/2 and 1/1/0.75, respectively [22].

In Geant4 simulations the thyroid was considered as a volumetric source in which ^{131}I is distributed uniformly. The ^{131}I γ-spectrum has peak energy of 0.365 MeV with 0.853 emission probability and 0.389 MeV energy per transformation, while beta spectra have an average energy of 0.183 MeV per transformation [23]. In our simulations we considered total energy per transformation. The term Iodine spectrum means dose rate contribution from gamma total energy per transformation and average beta energy per transformation. For absorbed fraction and S-values, the mass of thyroid was considered to be 1, 2, 4, 6, 8, 10 and 20 g respectively.

In order to keep the statistical uncertainties associated with the presented estimated results below 1%, 10^6 histories were generated for each simulated run, a value lower than the experimental uncertainty. Simulated dose rate was calculated using the following relation [24]:

$$\dot{D}=\frac{A\times E\times C}{N\times M}, \tag{2}$$

where $\dot{D}$ is the absorbed dose rate in Gy/hr, E is the deposited energy in Joules (J), A is the source activity in Bq, C is the conversion factor ($C=36\times 10^5$), N is the number of histories generated, and M is the detector mass in g.

3 Results

Geant4 simulations were carried out for various thyroid geometries and the estimated results were compared with the already published data [11]. Fig. 1 (at the bottom) shows the variation of the total energy deposition per decay of ^{131}I for both beta and gamma rays with the volume of thyroid, for various geometries.

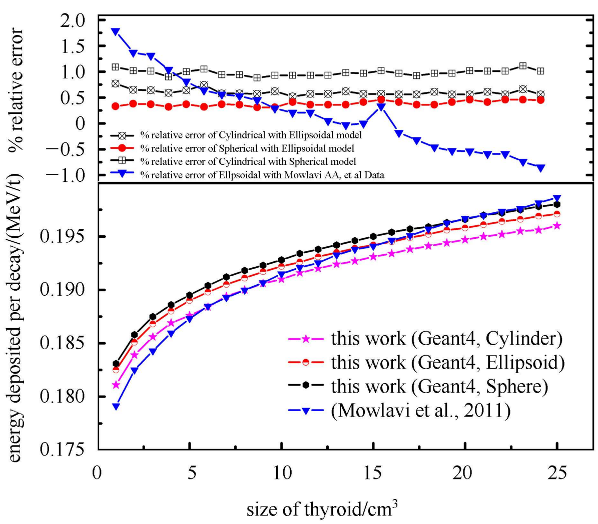

Fig. 1. Comparison of total energy deposition per decay for various geometries approximating thyroid in Geant4 studies with the corresponding results obtained with MCNP for various values of thyroid volume, shown at the bottom of the figure and percentage error of Geant4 results with different models and Mowlavi, et al., [12] results, shown at the top of the figure.

The relative differences ($\Delta E=(E_{\text{case}}-E_{\text{ref}})/E_{\text{ref}}$) against specified reference in each case, among various thyroid models considered in this study and results of Mowlavi et al., [12] are given at the top of Fig. 1.

In this study, besides the volume (η) variation of the thyroid, a variety of materials were also considered and the variation of the total energy deposition per decay (ϵ) for water, ICRP, and ICRU soft tissues were estimated, the corresponding results are shown in Fig. 2. The relative differences of water with ICRP and ICRU soft tissues, and between ICRP and ICRU soft tissues are shown in Fig. 2 (top of figure).

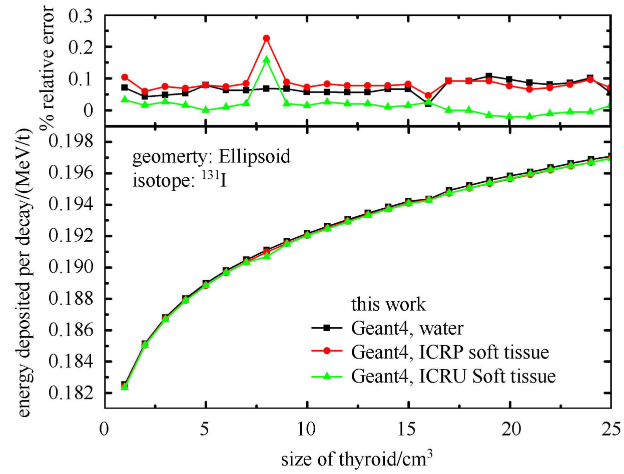

Fig. 2. (color online) Variation of total energy deposition per decay for water, ICRP and ICRU soft tissues with the thyroid volume (Shown at the bottom) and the percentage error of the Geant4 results for different tissues indicated composition (shown at the top).

The variation of energy deposition per decay per gram (ξ) with thyroid volume (η) for ellipsoidal geometry of thyroid is depicted in Fig. 3.

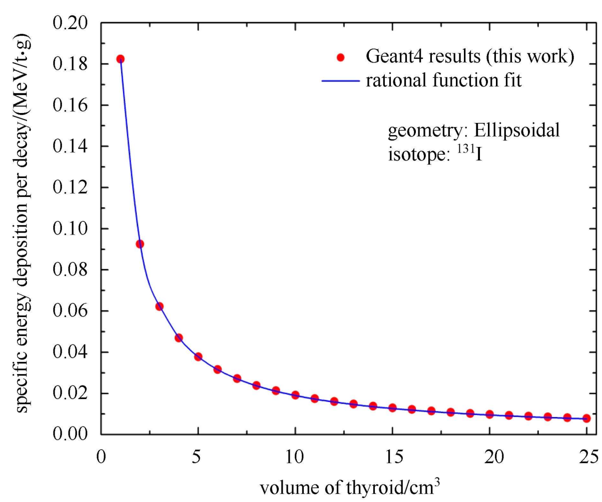

Fig. 3. Variation of energy deposition per decay per gram with the volume of thyroid.

The activity-to-dose-rate conversion factor K has also been calculated. Fig. 4 shows the dependence of K with thyroid volume.

The Geant4 estimated results of S-values for various thyroid geometries are given in Table 1. Comparison has been made for each model with published results [12].

Comparison of the Geant4 based S-values (given in Tables 2 and 3) for newborn, 1 year, 5 years, female and male with the corresponding MCNP, ICRP and ORNL data.

Absorbed fraction values for β-particles of ^{131}I, have also been estimated for various thyroid models and varying volumes, shown in Table 4. Geant4 based absorbed fraction results are compared with the already published results of Siegel and Stabin [12].

Similarly, the Geant4 estimated results of absorbed fraction for ^{131}I γ-rays, for spherical thyroid model are shown in Table 5. Comparison of Geant4 results were made with MIRD Pamphlet 8 (MIRD8), EGS4 and MCNP published results [14].

Table 1. S-values for different thyroid models and sizes, and comparison with Siegel and Stabin results.

	S-values/(rad/μCi-hr)						
mass/g	Ellipsoid	Siegel and Stabin	% relative diff of Ellipsoid with Siegel and Stabin	Sphere	% relative diff of Sphere with Siegel and Stabin	Cylinder	% relative diff of Cylinder with Siegel and Stabin
1	0.389	0.390	0.308	0.390	−0.077	0.386	1.026
2	0.197	0.200	1.400	0.198	1.000	0.196	2.000
4	0.100	0.100	−0.100	0.101	−0.500	0.100	0.400
6	0.067	0.069	2.319	0.068	2.029	0.067	3.043
8	0.051	0.052	2.115	0.051	1.731	0.051	2.692
10	0.041	0.042	2.619	0.041	2.143	0.041	3.095
20	0.021	0.021	0.952	0.021	0.000	0.021	1.429

Table 2. Comparison of the S-values calculated using Geant4 (this work) with published data for various values age of individual.

age	S-values/(Sv·Bq^{-1}·s^{-1})			ratios	
	this work (Geant4)	Ulanovsky et al (MCNP)	ICRP	Geant4/ MCNP	Geant4/ICRP
newborn	2.55E-11	2.26E-11	2.44E-11	1.13	1.05
1 year old	1.91E-11	1.64E-11	1.78E-11	1.17	1.07
5 year old	9.96E-12	8.67E-12	9.28E-12	1.15	1.07

Table 3. Gender based comparison of the calculated S-values using Geant4 (this work) with the published data.

gender	S-values/(Sv·Bq^{-1}·s^{-1})				ratios		
	Geant4	ICRP voxel phantoms	UF hybrid phantoms	ORNL stylized phantoms	Geant4/ICRP	Geant4/UF	Geant4/O RNL
female	2.01E-12	1.90E-12	1.90E-12	1.90E-12	1.06	1.06	1.06
male	1.56E-12	1.60E-12	1.70E-12	1.60E-12	0.98	0.92	0.98

∗Where Abbreviation E stands for power of 10

Table 4. Absorbed fraction for beta particles for different thyroid models, and sizes and comparison with siegel and stabin [13] results.

mass/g	Siegel and Stabin	Geant4 Ellipsoid	Geant4 Ellipsoid/ Siegel and Stabin	Geant4 Sphere	Geant4 Sphere/ Siegel and Stabin	Geant4 Cylinder	Geant4 Cylinder/ Siegel and Stabin
1	0.950	0.968	1.019	0.970	1.021	0.962	1.013
2	0.960	0.974	1.015	0.976	1.017	0.969	1.009
4	0.970	0.980	1.010	0.982	1.012	0.976	1.006
6	0.980	0.982	1.002	0.984	1.004	0.978	0.998
8	0.980	0.984	1.004	0.985	1.005	0.981	1.001
10	0.980	0.985	1.005	0.987	1.007	0.982	1.002
20	0.980	0.988	1.008	0.989	1.009	0.986	1.006

Table 5. Absorbed fraction for gammas using Geant4 Sphere and comparison with MIRD8, EGS4 and MCNP codes.

mass/g	this work (Geant4,Sphere)	MIRD8	EGS4	MCNP	MCNP/Geant4	EGS4/Geant4	Geant4/MIRD8
1	0.014	0.011	0.015	0.015	1.047	1.047	1.303
2	0.018	0.014	0.019	0.018	0.981	1.035	1.311
4	0.023	0.018	0.024	0.023	0.991	1.034	1.290
6	0.027	0.020	0.027	0.026	0.975	1.012	1.334
8	0.029	0.023	0.030	0.029	0.984	1.018	1.281
10	0.031	0.025	0.032	0.032	1.016	1.016	1.260
20	0.040	0.031	0.041	0.040	0.999	1.024	1.292

4 Discussions

The total energy deposition per decay increases with volume, because of the increasing volume-to-surface ratio for each type of model employed. The increase in volume of thyroid causes the fraction of radiations escaping from the thyroid to decrease, thereby increasing the absorbed energy of radiations. However, the slight difference in the total energy deposition per decay, for the cylindrical model, is due to the small value of the volume-to-surface ratio, which results in higher escape rates from the cylindrical model, as compared to elliptical and spherical models. The Geant4 results show a good agreement with already published results [11]. At smaller thyroid sizes the discrepancy between the Geant4 ellipsoid energy absorbed per decay and the results in Ref. [11] is large but as the size increases the difference becomes smaller.

The maximum relative differences in the results of various thyroid models considered in this study and the results of Mowlavi et al. [12] are up to 1.870%. The differences in the basic physics data sets used in MCNP and Geant4 simulation codes, as well as the different treatments of radiation transport (especially of β-radiations), may contribute towards the observed discrepancies.

The energy depositions per decay for various models of the thyroid are estimated, which can easily be converted into absorbed dose, knowing the mass and activity of the thyroid. From the relative differences, it is clear that treating volume- and/or mass- of thyroid constant results in an underestimation of the organ dose. Therefore, accurate assessment of thyroid volume is essential for exact therapeutic dose calculations for efficient treatment of the patients treated with ^{131}I.

A comparison of the dosimetric properties of water with different tissue compositions is useful for validating its use in radiation dosimetry. The maximum relative difference among the Geant4 estimated results for water with ICRP and ICRU soft tissues is 0.107% and 0.225%, respectively, while between ICRP and ICRU soft tissues this maximum difference is 0.157%. In either case the maximum difference in not greater than 0.225%. The water, ICRP, and ICRU soft tissue materials have the same atomic densities but different atomic compositions. It has been shown by Ellett and Humes [25] that, for photons with energy values less than 100 keV, the absorbed fraction is increasingly sensitive to atomic composition. On the basis of relative differences among the three materials, it is suggested that water can be used as a phantom material in place of ICRP and ICRU tissues, for dosimetric purposes. The Geant4 computed variation of total energy deposition per decay (ϵ) with volume of thyroid (η) for water, follows parametric power fit:

$$\epsilon=a(1+\eta)^b, \tag{3}$$

with parameters a, b having values $0.179\pm8.8\times10^{-5}$ and $0.029\pm1.9\times10^{-4}$, respectively, with $R^2=0.999$.

The variation of energy deposition per decay per gram (ξ) with thyroid volume (η) for ellipsoidal geometry of thyroid is depicted in Fig. 3. With the increase in thyroid volume, the value of ξ decreases following the parametric rational fit:

$$\xi=\frac{1}{a+b\eta}, \tag{4}$$

where, a, b are fitting parameters with values 0.249 ± 0.079 and 5.239 ± 0.015, respectively, with $R^2=0.999$. The therapist must accurately determine the volume of the thyroid so that the precise amount of ^{131}I must be administered to the patient for a prescribed dose to thyroid, as recommended for the specific protocol.

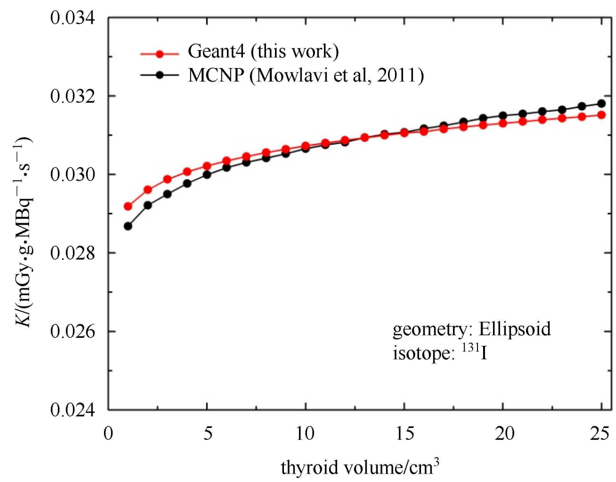

Fig. 4. Comparison of Geant4 computed values of K (mGy·g·MBq^{-1}·s^{-1}) with the corresponding MCNP based data [12] for various values of thyroid volume.

In the literature, such as MIRDOSE code, the activity-to-dose-rate conversion factor, K, has a value of 0.0313 (mGy·g·MBq^{-1}·s^{-1}) [26], calculated by MC method for gamma rays with the assumption that beta particle deposit their full energy within the thyroid (spherical geometry with fixed mass of 10 g). It can be seen in Fig. 4 that K has a significant difference with typical considered constant value, the difference varies from −6.741% to 0.703% for volume variation of 1 to 25 cm^3. For a 10 g thyroid lobe, our calculation shows a difference of nearly 1.8% with MIRDOSE3 value of K. In Fig. 4, an excellent agreement of Geant4 ellipsoidal results with published data [11] using MCNP simulation code is evident. The Geant4 results differ in the range of −0.881 to 1.778% from corresponding result of MCNP for the volume variation of 1 to 25 cm^3. From the results, it can be seen that there is some difference in MIRD and Geant4 results. The reason for the difference is mainly due to the following factors: the first factor is the spectrum used for simulation [14]; the second factor is due to detailed consideration of beta and gamma transport in and out of thyroid, and may also be due to differences in interaction probability database used in the two simulation codes. The activity-to-dose-rate conversion factor K has the following fitted dependence on thyroid volume (η):

$$K=a(1+\eta)^b, \tag{5}$$

with parameters a, b having values $0.0287\pm1.4\times10^{-5}$ and $0.0289\pm1.9\times10^{-4}$ respectively with $R^2=0.998$.

The Geant4 based estimated S-values for spherical, ellipsoidal and cylindrical thyroid geometries are presented here for comparison with each other and with the already published results [12]. Siegal and Stabin evaluated S-values and absorbed fractions for electron and β-sources uniformly distributed within spheres of various sizes using the methodology developed earlier [13]. The maximum relative difference of ellipsoidal, spherical, and cylindrical geometries with Siegel and Stabin results were 2.619, 2.143 and 3.095%, respectively. The observed difference may be attributed to the differences in interaction probability databases used in the Berger's method and in Geant4 Standard physics model. Other contributing factors may include the lack of scattering of radiations from the surrounding tissue in the study performed Siegel and Stabin. The Geant4 model used in this work takes into account all such scatterings. Moreover, the Geant4 model performs simulations using the full β- and γ-transport in our calculation. Comparison of the Geant4 based S-values (given in Table 2 and 3) for Newborns, 1 year, 5 years, females and males show an excellent agreement with the corresponding MCNP, ICRP and ORNL data.

The absorbed fraction is an important dosimetric quantity used in radiation oncology etc. In any dosimetric analysis, the first term to be evaluated is the absorbed fraction, depending on the radionuclide characteristic, shape, size and location of target volume. In this study, the absorbed fraction values for β-particles of ^{131}I, have been estimated for various thyroid models. The results are compared with data published by Siegel and Stabin [12]. The maximum relative difference of ellipsoidal, spherical and cylindrical geometries with Siegel and Stabin results are 1.860, 2.105 and 1.263%, respectively. It is also observed that with the increase of size of thyroid the relative difference reduces. For a smaller organ size, the β-particles range is large, relative to the organ dimension; therefore, an appreciable amount of energy escapes beyond the organ boundaries. In the traditional models, the absorbed fraction for β-particles is assumed to be unity for the source organ and zero elsewhere. This may be reasonable for most situations and even for relatively small organs like thyroid because the range of most β-particles in body tissues is small compared to the size of most source regions. However, in this study we consider the thyroid as a volumetric source, the absorbed fraction is not unity for larger thyroid sizes because some of the β-particles escape from nearby surfaces, consequently decreasing the absorbed fraction.

Similarly absorbed fraction values for ^{131}I γ-rays have also been estimated using spherical thyroid geometry and the results are compared with MIRD8, EGS4 and MCNP published data [14]. The Geant4 results were again in good agreement with MCNP and EGS4 but produced results that differed from the values published in MIRD8. The Geant4 estimated results were typically 24%–29.032% higher than those in MIRD8 for most values of thyroid volumes. The maximum relative difference of Geant4 results with EGS4 and MCNP is 6.667% for each case. Since the contribution of gamma photons in the S-values is ∼2%, this effects the over-all deviation of S-values slightly.

5 Conclusions

This study shows that the Geant4 code can be used effectively for internal dosimetry of the thyroid and from the results. The following conclusions may be drawn:

1) Geant4 based calculations of energy deposition per decay and the S-values for spherical, ellipsoidal, and cylindrical models of human thyroid are in excellent agreement with the corresponding results obtained by using MCNP and the moment based analytical techniques.

2) Variation of absorbed fraction and S-values with mass clearly indicates that keeping the thyroid volume/mass during ^{131}I therapy may underestimate the absorbed dose.

3) The variation of energy deposition per decay with size of thyroid clearly shows that water can safely be used to model ICRP- and ICRU-based tissue materials for thyroid.

4) The size dependent specific energy deposition per decay can be estimated by using rational fitting formula with values of parameters as $a=0.249\pm0.079$ and 5.239 ± 0.015 for thyroid.

5) For the thyroid volume range of 1–25 cm^3 studied in this work, the Geant4 based estimated values of the k-factor show good agreement with the corresponding MCNP based data.

6) For γ-absorbed fractions, the Geant4 results remain close to the corresponding EGS4 and MCNP data within 6.667%, whereas discrepancies upto 29.032% are observed with the MIRD based results.

7) The value of β-absorbed fractions for various geometries of thyroid used in Geant4 show good agreement with already published data with deviations remaining with 2.105%.

References

1 Lassmann M et al. Endicrine-Related Cancer, 2010, **17**: R161-R172
2 Haugen B R. Seminars in Surgical Oncology, 1999, **16**: 34–41
3 Jentzen W et al. European Journal of Nuclear Medicine and Molecular Imaging, 2010, **37**: 884–895
4 Clarke S E M. Clinical Oncology, 2010, **22**: 430–437
5 Freudenberg M W R, Kotzerke J. Z. Med. Phys., 2011, **21**: 9
6 Tuttle R M et al. Journal of Nuclear Medicine, 2006, **47**: 1587–1591
7 Haq M S et al. Nuclear Medicine Communications, 2004, **25**: 799–805
8 Stabin M G, Flux G D. Biomedical Imaging & Intervention Journal, 2007, **3**: e28
9 Barca F C G, Chauvie S, Cuce D. Nuclear Physics B, 2003, **125**: 5
10 Meo S L et al. Nuclear Medicine Communications, 2008, **29**: 1100–1105
11 Mowlavi A A et al. Radiology and Oncology, 2011, **45**: 143–146
12 Siegel J A, Stabin M G. Journal of Nuclear Medicine, 1994, **35**: 152–156
13 Berger M J. Journal of Nuclear Medicine, 1971, **12**: 5–23
14 Stabin M G, Konijinenberg M W. Journal of Nuclear Medicine, 2000, **41**: 149–160
15 Bogazzi F et al. Journal of Clinical Endocrinology & Metabolism, 1999, **84**: 499–503
16 Chiovato L et al. Journal of Clinical Endocrinology & Metabolism, 1998, **25**: 40–46
17 Peters H et al. Euorpean Journal of Clinical Investigation, 1996, **26**: 59–63
18 Traino A C et al. Physics in Medicine and Biology, 2000, **45**: 121–129
19 Grosev D et al. Nuklearmedizin, 2008, **47**: 120–126
20 Agostinelli S et al. Nuclear Instruments and Methods in Physics Research Section A: Accelerators, Spectrometers, Detectors and Associated Equipment, 2003, **506**: 250–303
21 Allison J et al. IEEE Transactions on Nuclear Science, 2006, **53**: 270–278
22 Brownell G L et al. Journal of Nuclear Medicine, 1968, **9**: 27–39
23 Cember H. Introduction to Health Physics: McGraw-Hill, Health Professions Division, 1996
24 Kadri O et al. Applied Radiation and Isotopes, 2006, **64**: 170–177
25 Ellen W H, Humes R M. MIRD Pamphlet 8, Journal of Nuclear Medicine, 1971, **12**: 25–32
26 Stabin M G. Journal of Nuclear Medicine, 1996, **37**: 538–546